Quantum Electronics Letters

Femtosecond Self-Doubling Optical Parametric Oscillator Based on KTiOAsO$_4$

Tolga Kartaloğlu and Orhan Aytür

Abstract—We report a femtosecond intracavity-frequency-doubled optical parametric oscillator that employs a single KTiOAsO$_4$ crystal for both parametric generation and frequency doubling. This device generates a yellow output beam at 575 nm with 39.4% power conversion efficiency when synchronously pumped by a femtosecond Ti:sapphire laser at a wavelength of 796 nm. An intracavity retarder is employed to alleviate temporal pulse overlap problems associated with group velocity mismatch inside the KTiOAsO$_4$ crystal.

Index Terms—Nonlinear frequency conversion, optical parametric oscillators, parametric devices, second harmonic generation (SHG).

I. INTRODUCTION

IN RECENT years, there has been a growing interest in second-order nonlinear wavelength conversion systems that utilize the simultaneous phase matching of two different processes within the same nonlinear crystal [1]–[24]. Efficient wavelength conversion of lasers to wavelengths that cannot be reached via a single nonlinear process have been demonstrated with such systems [1]–[13]. In particular, self-doubling optical parametric oscillators (SD-OPOs), where optical parametric oscillation and second-harmonic generation (SHG) are simultaneously phase-matched within the same nonlinear crystal, were shown to provide efficient tunable upconversion of near-infrared lasers to visible wavelengths [1]–[5]. Even though the same wavelength range can be reached by cascading an optical parametric oscillator (OPO) and a SHG crystal (either external or internal to the OPO cavity), the conversion efficiency of the two-step process is usually low, and the presence of a second crystal increases system complexity.

In a SD-OPO, the signal beam propagating through the nonlinear crystal experiences gain due to parametric amplification and draws power from the pump beam, but at the same time experiences loss due to SHG and loses power to the second-harmonic beam. The high-finesse OPO cavity that is singly resonant at the signal wavelength typically has very low parasitic linear losses. These parasitic losses are compensated for by the net gain (parametric gain minus loss due to SHG) experienced by the signal beam. The second-harmonic beam is coupled out of the cavity with the use of a dichroic beamsplitter.

An analysis of simultaneous phase matching of OPO and SHG interactions has identified a number of different polarization geometries for SD-OPOs [18]. When type-II phase-matched SHG is employed, it is necessary to rotate the polarization of the intracavity signal beam to allow simultaneous SHG. This is actually advantageous, since it provides an externally adjustable parameter, namely the polarization rotation angle, that can be used to optimize the conversion efficiency for the particular pump power at hand. These issues are analyzed extensively in [18].

In this paper, we report a femtosecond SD-OPO in which a single KTiOAsO$_4$ (KTA) crystal is employed for both parametric generation and SHG. The SD-OPO is synchronously pumped by a Ti:sapphire
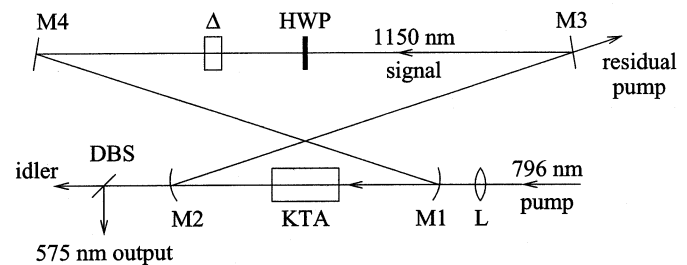
Fig. 1. Experimental setup of the SD-OPO. A mode-locked Ti:sapphire laser at a wavelength of 796 nm provides the pump beam.

laser operating at a wavelength of 796 nm. Noncritical type-II birefringent phase matching in the KTA crystal leads to a signal beam at 1150 nm. Simultaneously phase-matched frequency doubling of the intracavity signal beam within the same KTA crystal is facilitated by intracavity rotation of the signal polarization. The resulting yellow beam at 575 nm exits the cavity via a dichroic beamsplitter. A fixed time delay introduced between the two orthogonally polarized intracavity signal pulses is shown to alleviate temporal pulse overlap problems associated with group velocity mismatch (GVM). The overall (from 796 to 575 nm) power conversion efficiency of the two step process is 39.4%. To our knowledge, this is the highest value reported to date for an intracavity frequency-doubled OPO.

II. EXPERIMENTAL SETUP

Our SD-OPO is based on a 20-mm-long KTA crystal that is cut for noncritical phase matching along the $\theta = 90°$ and $\phi = 0°$ direction. A type-II polarization geometry is employed to achieve parametric generation, where both the pump at 796 nm and the signal at 1150 nm are p-polarized (horizontal, fast axis, y axis), and the idler is s-polarized (vertical, slow axis, z axis). Frequency doubling of the signal beam is also type-II phase-matched for the same direction of propagation; the fundamental beam at 1150 nm has both p- and s-polarized components, and the second-harmonic beam at 575 nm is p polarized. This polarization geometry belongs to class-C SD-OPOs, as defined in [18]. The crystal has antireflection coatings for the signal, pump, and second-harmonic wavelengths on both surfaces.

Our experimental setup shown in Fig. 1 is based on a ring cavity made up of four mirrors that are high reflectors at the signal wavelength. Mirrors M1 and M2 are 100-mm radius-of-curvature concave, and M3 and M4 are flat. The lowest order transverse mode of the cavity forms an intracavity focus with a diameter of 30 μm (calculated) between M1 and M2 with the KTA crystal placed at the focus. The fast axis of the crystal is parallel to the horizontal plane coinciding with the polarization of the pump beam. A mode-locked Ti:sapphire laser that has 140-fs-long pulses (216-fs autocorrelation) at a repetition rate of 76 MHz provides the pump beam at a wavelength of 796 nm. The pump beam is focused with a lens (L) of focal length 50 mm and enters the cavity through M1. The focused pump beam has a 62-μm diameter (measured). An intracavity half-wave plate (HWP) is used to couple a portion of the p-polarized signal beam to s-polarization to facilitate type-II phase-matched SHG. Synchronization of the p-polarized intracavity signal pulses with the pump pulses is achieved by moving M3 with a piezo-electrically controlled mount. The frequency-doubled yellow beam at 575 nm exits the cavity through M2, which is coated for high-transmission at this wavelength and high reflection at the pump

wavelength. This optic is also transparent to the idler beam at 2586 nm. An external dichroic beamsplitter (DBS) is used to separate the output yellow beam from the idler beam. The diverging output beam is collimated with a lens (not shown). The residual pump beam leaves the cavity through M3.

After the intracavity signal polarization is rotated with the HWP, a birefringent crystal is used as a retarder (Δ) to provide a fixed time delay between the s- and p-polarized components of the signal beam, with the intention of achieving better temporal overlap between these pulses inside the KTA crystal. If this time delay were not present, the two orthogonally polarized signal pulses would enter the crystal synchronously, and start walking away from each other due to GVM. (The calculated GVM for these pulses is 300 fs/mm.) However, the retarder provides a fixed time delay of 1.48 ps, so that the s-polarized signal pulse leads the p-polarized signal pulse by approximately 0.45 mm before entering the crystal. Once inside the crystal, the p-polarized pulse catches up with the s-polarized pulse approximately 5 mm from the input facet. This arrangement essentially doubles the effective crystal length that is available for SHG.

The particular birefringent crystal that we use as a retarder is a 5-mm-long KTP crystal that is cut in the $\theta = 90°$ and $\phi = 0°$ direction. Its polarization axes are oriented so that the slow axis is p-polarized and the fast axis is s-polarized, opposite to those of the KTA crystal. Since in this orientation and at the present wavelengths this KTP crystal is not phase matched for any second-order interaction, its nonlinear nature does not come into play, and its effect is limited to linear retardation between orthogonal polarization components at the signal wavelength.

III. RESULTS AND DISCUSSION

In the intracavity-doubled OPO, the resonant intracavity signal power is coupled out of the cavity by means of nonlinear SHG. When there is no intracavity polarization rotation (either the HWP is removed from the cavity or its fast and slow axes are aligned with those of the KTA crystal), the intracavity signal beam does not have an s-polarized component, resulting in little frequency doubling (only due to parasitic interactions). In this case, the OPO is severely undercoupled, and the intracavity signal power is very high. The threshold of this undercoupled OPO is 51 mW. At an input pump power of 655 mW, the pump beam is depleted by 87%, showing strong parametric conversion.

As we start rotating the intracavity signal polarization by rotating the HWP, a portion of the p-polarized intracavity signal is coupled into s-polarization, and phase-matched SHG begins to take place. Fig. 2 shows the output second-harmonic power at 575 nm as a function of the intracavity polarization rotation angle. Both polarization components at the signal wavelength get depleted due to SHG in the crystal, reducing the resonant intracavity signal power. As the polarization rotation angle is increased, the second-harmonic output power increases up to a maximum, and then begins to decrease as a consequence of reduced intracavity signal power. Rotating the signal polarization effectively increases linear cavity losses as well, and the OPO falls below threshold at one point. At 655-mW pump power, the second-harmonic output power reaches a maximum value of 258 mW at a polarization rotation angle of 22°, and the OPO falls below threshold at 54°. At the maximum point, the power conversion efficiency from the input pump beam to the output second-harmonic beam is 39.4%, and the pump depletion is 82%. We note that, in this case, the s-polarized signal component is completely depleted at the exit facet of the crystal.

Since two 796-nm photons are annihilated to create one 575 nm photon, the photon conversion efficiency for the SD-OPO is defined as the number of output 575-nm photons divided by half the number of input 796-nm photons. (Full conversion yielding a photon conversion efficiency of 100%.) Our 39.4% power conversion efficiency cor-
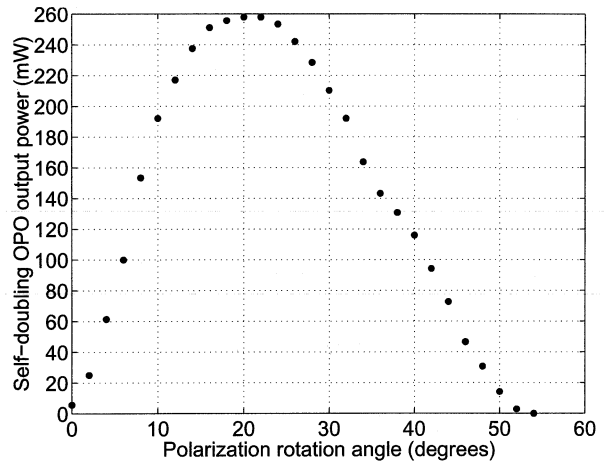

Fig. 2.   SD-OPO output power at 575 nm as a function of polarization rotation angle.
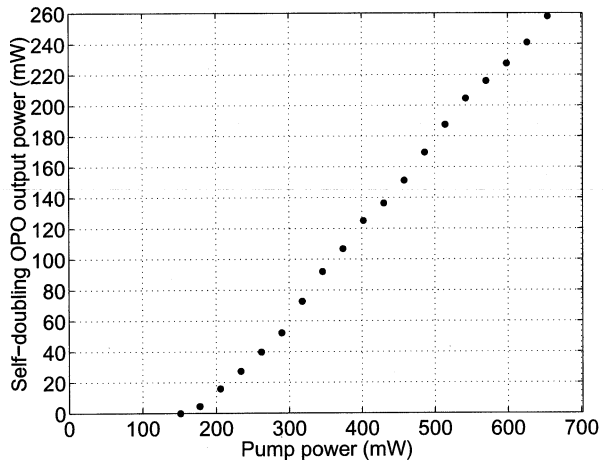

Fig. 3.   SD-OPO output power at 575 nm as a function of input pump power while the retarder rotation angle is held fixed at 22°.

responds to a photon conversion efficiency of 56.4%. Fig. 3 shows the output second-harmonic power as a function of input pump power at a constant polarization rotation angle of 22°. In this case, the OPO threshold is 151 mW. Note that the power input–output graph of Fig. 3 is far from being saturated at high-input power levels.

The spectrum of the yellow output beam as measured by a monochrometer (resolution 0.5 nm) is shown in Fig. 4. The output spectrum is narrower than those of the pump and the intracavity signal. The autocorrelation width of the yellow output pulses is measured to be 789 fs. This pulse broadening is due to both GVM in the KTA crystal and group velocity dispersion (GVD) in the KTA and retarder crystals. We used an external two-prism double-pass pulse compressor composed of two SF-10 isosceles Brewster prisms that are separated by 108 cm, and reduced the autocorrelation width of the output to 318 fs. Fig. 5 shows the autocorrelation of the output pulses before and after the pulse compressor. Unfortunately, unlike pulse broadening due to GVD, broadening due to GVM cannot be reversed using an external compressor. Hence, the output pulses are still not transform limited after compression. Assuming secant hyperbolic (sech) pulse shapes, the pulses are estimated to be 6.2- and 2.5-times transform limited, before and after the pulse compressor, respectively. The transverse profile of the yellow output beam as measured with a CCD camera is nearly Gaussian.

In principle, it is possible to tune the output wavelength of this SD-OPO by varying the KTA crystal angles in conjunction with the pump wavelength. We could not demonstrate this in practice, however, due to the narrow clear aperture (4 mm) of our relatively long crystal (20 mm). Using
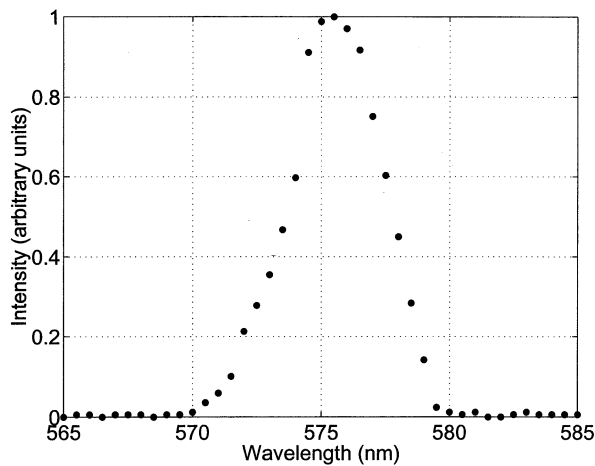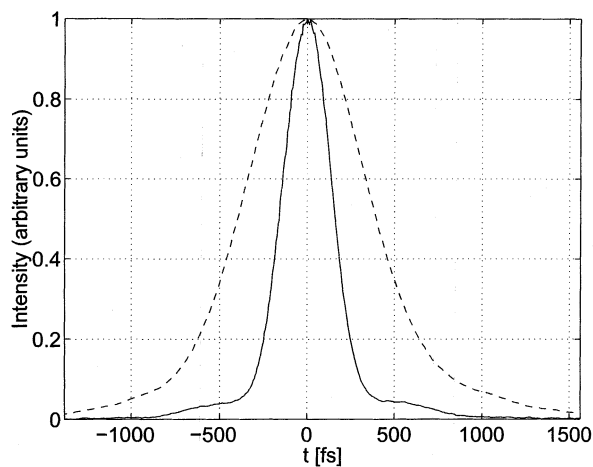
Fig. 4.   Spectrum of the SD-OPO output.

Fig. 5.   Autocorrelation traces of the SD-OPO output before (dashes line) and after (solid line) external pulse compression.

a crystal with a larger clear-aperture-to-length ratio, it should be possible to rotate the crystal up to approximately $65°$ in either direction (corresponding to a $30°$ internal angle) without too much degradation in the performance of the anti-reflection coatings on the crystal facets. We calculated that it is possible to tune this SD-OPO between 575 and 696 nm by varying θ in the $90°$ to $60°$ range (internal) and the pump wavelength in the 796- to 825-nm range. Similarly, changing ϕ from $0°$ to $30°$ (internal) and the pump wavelength from 796 to 792 nm, it is possible to tune the output from 575 to 566 nm.

IV. CONCLUSION

We have demonstrated a SD-OPO that employs a single KTA crystal for both parametric generation and frequency doubling. The two-step conversion from the pump wavelength to the second-harmonic of the signal wavelength is very efficient. Providing a delay between the two orthogonally polarized signal components to partially alleviate GVM effects contributes to this high efficiency. To our knowledge, our conversion efficiency from the pump to the second-harmonic is the highest value reported to date for an intracavity frequency-doubled OPO.

REFERENCES

[1] T. Kartaloğlu, K. G. Köprülü, and O. Aytür, "Phase-matched self-doubling optical parametric oscillator," *Opt. Lett.*, vol. 22, pp. 280–282, 1997.

[2] C. McGowan, D. T. Reid, Z. E. Penman, M. Ebrahimzadeh, W. Sibbett, and D. H. Jundt, "Femtosecond optical parametric oscillator based on periodically poled lithium niobate," *J. Opt. Soc. Amer. B*, vol. 15, pp. 694–701, 1998.

[3] T. Kartaloğlu, Z. G. Figen, and O. Aytür, "A self-doubling optical parametric oscillator based on aperiodically-poled lithium niobate," in *Proc. 2001 IEEE/LEOS Annual Meeting Conf.*, 2001, pp. 243–244.

[4] X. P. Zhang, J. Hebling, J. Kuhl, W. W. Rühle, and H. Giessen, "Efficient intracavity generation of visible pulses in a femtosecond near-infrared optical parametric oscillator," *Opt. Lett.*, vol. 26, pp. 2005–2007, 2001.

[5] S. D. Butterworth, P. G. R. Smith, and D. C. Hanna, "Picosecond Ti : sapphire-pumped optical parametric oscillator based on periodically poled LiNbO₃," *Opt. Lett.*, vol. 22, pp. 618–620, 1997.

[6] K. G. Köprülü, T. Kartaloğlu, Y. Dikmelik, and O. Aytür, "Single-crystal sum-frequency generating optical parametric oscillator," *J. Opt. Soc. Amer. B*, vol. 16, pp. 1546–1552, 1999.

[7] M. Vaidyanathan, R. C. Eckardt, V. Dominic, L. E. Myers, and T. P. Grayson, "Cascaded optical parametric oscillations," *Opt. Exp.*, vol. 1, pp. 49–53, 1997.

[8] V. Petrov and F. Noack, "Frequency upconversion of tunable femtosecond pulses by parametric amplification and sum-frequency generation in a single nonlinear crystal," *Opt. Lett.*, vol. 20, pp. 2171–2173, 1995.

[9] C. Zhang, H. Wei, Y. Y. Zhu, H. T. Wang, S. N. Zhu, and N. B. Ming, "Third-harmonic generation in a general two-component quasiperiodic optical superlattice," *Opt. Lett.*, vol. 26, pp. 899–901, 2001.

[10] G. Z. Luo, S. N. Zhu, J. L. He, Y. Y. Zhu, H. T. Wang, Z. W. Liu, C. Zhang, and N. B. Ming, "Simultaneously efficient blue and red light generations in a periodically poled LiTaO₃," *Appl. Phys. Lett.*, vol. 78, pp. 3006–3008, 2001.

[11] Y. Q. Qin, Y. Y. Zhu, S. N. Zhu, and N. B. Ming, "Quasiphase-matched harmonic generation through coupled parametric processes in a quasiperiodic optical superlattice," *J. Appl. Phys.*, vol. 84, pp. 6911–6916, 1998.

[12] Y. Q. Qin, Y. Y. Zhu, S. N. Zhu, G. P. Luo, J. Ma, and N. B. Ming, "Nonlinear optical characterization of a general Fibonacci optical superlattice," *Appl. Phys. Lett.*, vol. 75, pp. 448–450, 1999.

[13] Y. B. Chen, C. Zhang, Y. Y. Zhu, S. N. Zhu, H. T. Wang, and N. B. Ming, "Optical harmonic generation in a quasiphase-matched three-component Fibonacci superlattice LiTaO₃," *Appl. Phys. Lett.*, vol. 78, pp. 577–579, 2001.

[14] Y. Y. Zhu, R. F. Xiao, J. S. Fu, G. K. L. Wong, and N. B. Ming, "Third harmonic generation through coupled second-order nonlinear optical parametric processes in quasiperiodically domain-inverted Sr₀.₆Ba₀.₄Nb₂O₆ optical superlattices," *Appl. Phys. Lett.*, vol. 73, pp. 432–434, 1998.

[15] K. F. Kashi, A. Arie, P. Urenski, and G. Rosenman, "Multiple nonlinear optical interactions with arbitrary wave vector differences," *Phys. Rev. Lett.*, vol. 88, no. 023 903, 2002.

[16] K. C. Burr, C. L. Tang, M. A. Arbore, and M. M. Fejer, "High-repetition-rate femtosecond optical parametric oscillator based on periodically poled lithium niobate," *Appl. Phys. Lett.*, vol. 70, pp. 3341–3343, 1997.

[17] O. Pfister, J. S. Wells, L. Hollberg, L. Zink, D. A. Van Baak, M. D. Levenson, and W. R. Bosenberg, "Continuous-wave frequency tripling and quadrupling by simultaneous three-wave mixing in periodically poled crystals: Application to a two-step 1.19–10.71-μm frequency bridge," *Opt. Lett.*, vol. 22, pp. 1211–1213, 1997.

[18] O. Aytür and Y. Dikmelik, "Plane-wave theory of self-doubling optical parametric oscillators," *IEEE J. Quantum Electron.*, vol. 34, pp. 447–458, Mar. 1998.

[19] Y. Dikmelik, G. Akgün, and O. Aytür, "Plane-wave dynamics of optical parametric oscillation with simultaneous sum-frequency generation," *IEEE J. Quantum Electron.*, vol. 35, pp. 897–912, June 1999.

[20] Y. Y. Zhu and N. B. Ming, "Dielectric superlattices for nonlinear optical effects," *Opt. Quantum Electron.*, vol. 31, pp. 1093–1128, 1999.

[21] K. F. Kashi and A. Arie, "Multiple-wavelength quasiphase-matched nonlinear interactions," *IEEE J. Quantum Electron.*, vol. 35, pp. 1649–1656, Nov. 1999.

[22] Y. B. Chen, Y. Y. Zhu, Y. Q. Qin, C. Zhang, S. N. Zhu, and N. B. Ming, "Second harmonic and third harmonic generation in a three-component Fibonacci optical superlattice," *J. Phys.: Condens. Matter*, vol. 12, pp. 529–537, 2000.

[23] S. Saltiel and Y. S. Kivshar, "Phase matching in nonlinear $\chi^{(2)}$ photonic crystals," *Opt. Lett.*, vol. 25, pp. 1204–1206, 2000.

[24] Y. Zhang and B. Y. Gu, "Optimal design of aperiodically poled lithium niobate crystals for multiple wavelengths parametric amplification," *Opt. Commun.*, vol. 192, pp. 417–425, 2001.